

# E-ELT Multi-Conjugate Adaptive Optics module

E. Diolaiti<sup>1,a</sup>, I. Foppiani<sup>1,2</sup>, J.-M. Conan<sup>3</sup>, R. C. Butler<sup>4</sup>, R. I. Davies<sup>5</sup>, A. Baruffolo<sup>6</sup>, M. Bellazzini<sup>1</sup>, G. Bregoli<sup>1</sup>, P. Ciliegi<sup>1</sup>, G. Cosentino<sup>2</sup>, B. Delabre<sup>7</sup>, T. Fusco<sup>3</sup>, N. Hubin<sup>7</sup>, M. Lombini<sup>1,2</sup>, E. Marchetti<sup>7</sup>, C. Petit<sup>3</sup>, C. Robert<sup>3</sup>, L. Schreiber<sup>2</sup>

<sup>1</sup>INAF-Osservatorio Astronomico di Bologna, via Ranzani 1, 40127 Bologna, Italy

<sup>2</sup>Università di Bologna - Dipartimento di Astronomia, via Ranzani 1, 40127 Bologna, Italy

<sup>3</sup>ONERA, DOTA-CC, 29 av. de la div. Leclerc, B.P. 72, 92322 Chatillon cedex, France

<sup>4</sup>INAF-Istituto di Astrofisica Spaziale e Fisica cosmica, via Gobetti 101, 40129 Bologna, Italy

<sup>5</sup>Max Planck Institut fuer extraterrestrische Physik, Postfach 1312, 85741 Garching, Germany

<sup>6</sup>INAF-Osservatorio Astronomico di Padova, vicolo dell'Osservatorio 5, 35122 Padova, Italy

<sup>7</sup>European Southern Observatory, Karl-Schwarzschild-Str. 2, 85748 Garching, Germany

**Abstract.** MAORY is the multi-conjugate adaptive optics module for the future European Extremely Large Telescope. This paper describes the design and estimated performance of the module after the phase-A study; in particular two optical design options of the MAORY post-focal relay are discussed.

## 1. Introduction

The future 40 meter class European Extremely Large Telescope (E-ELT, [1]) requires adaptive optics to fully achieve its scientific goals. MAORY [2] is a crucial adaptive optics facility as it will feed MICADO [3, 4], the E-ELT high angular resolution imager. MAORY is based on Multi-Conjugate Adaptive Optics (MCAO), a technique that has been demonstrated to work on sky by MAD [5] on VLT and by GeMS [6] on Gemini.

MAORY provides a corrected Field of View (FoV) of 120 arcsec diameter on the wavelength range 0.8-2.4 micron. Wavefront correction is carried out by the telescope's adaptive mirror M4, optically conjugated to the ground layer and complemented by the tip-tilt mirror M5, and by two Deformable Mirrors (DM) integrated in MAORY and conjugated to high altitude turbulent layers. Wavefront sensing is performed by a suite of six Laser Guide Star WaveFront Sensors (LGS WFS) and three Natural Guide Star WaveFront Sensors (NGS WFS) for the measurement of the modes which cannot be properly sensed by the LGS WFS. The MCAO system architecture is based on a robust approach, which ensures reliable peak performance as well as high sky coverage.

An overview of the module design and performance based on the phase-A study is given. The latest developments concerning the post-focal relay optical design are also shown.

---

<sup>a</sup> e-mail : emiliano.diolaiti@oabo.inaf.it

## 2. System design

The foreseen location of MAORY is the E-ELT Nasmyth platform, on one of the bent foci (Figure 1). The module feeds two focal stations: the gravity invariant port underneath the optical bench, providing mechanical derotation for MICADO, and the lateral port on one side of the bench to feed an instrument standing on the Nasmyth platform, detached from the module. A detailed view of the opto-mechanical layout of MAORY without enclosure is shown in Figure 2.

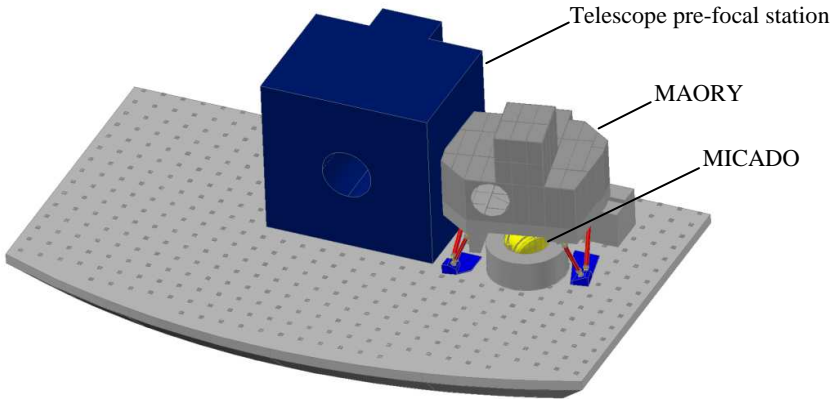


**Fig. 1.** Overall layout of MAORY on the E-ELT Nasmyth platform.

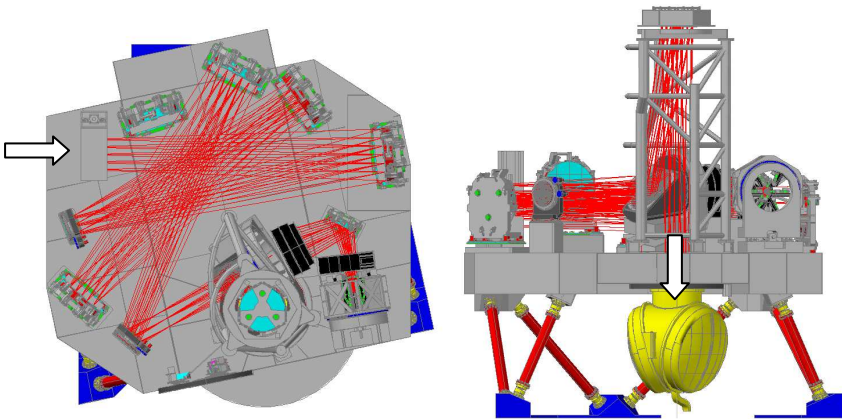


**Fig. 2.** Left: top view of the MAORY optical bench without enclosure. Right: lateral view. The MICADO cryostat is on the gravity invariant port below the bench. Arrows indicate the light path.

## Adaptive Optics for Extremely Large Telescopes II

From the optical design point of view, the post-focal relay of MAORY is a finite conjugate relay formed by two pairs of aspheric off-axis mirrors. Three flat mirrors fold the relay to fit the reserved area on the Nasmyth platform; two out of these flat mirrors are deformable and compensate the atmospheric turbulence. The optical relay makes an image of the telescope F/17.7 focal plane with unit magnification. The splitting of the science and LGS beams in the optical relay is accomplished by a dichroic, that transmits the LGS light (wavelength 0.589  $\mu\text{m}$ ) and reflects the science channel light (wavelengths longer than 0.6  $\mu\text{m}$ ). The LGS beam transmitted by the dichroic is focused by a refractive objective, that creates a F/5.1 focus, reducing the travel for refocusing when the zenith angle and the sodium layer range change. Assuming optical coatings based on multi-layer protected silver similar to those foreseen for the telescope, the thermal background of MAORY is expected to have an acceptable impact on MICADO: the thermal background integrated over the Ks band (central wavelength 2.16  $\mu\text{m}$ ) is less than 50% of the total background due to telescope and sky together at typical ambient temperature. For this reason MAORY is not cooled as a baseline.

The optical design of the post-focal relay, without folding mirrors, is shown in Figure 3-left. The two pairs of mirrors re-image the telescope focal plane with excellent optical quality, creating two intermediate pupil images. This design, although intrinsically simple, has some drawbacks. The output focus is characterized by considerable field curvature due to the use of only concave mirrors. Moreover the dichroic turns out to be rather large. Finally the LGS beams are aberrated by reflection onto three off-axis mirrors: the lenses of the LGS refractive objective (not shown in Figure 3) are wedged in order to achieve a reasonable wavefront error in the LGS path.

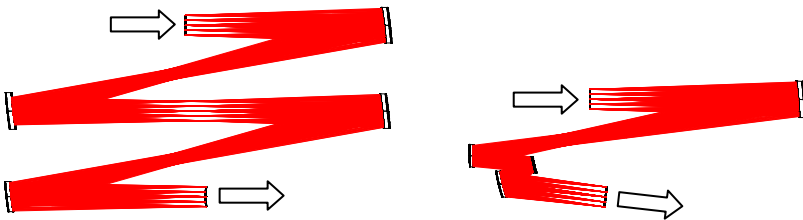


**Fig. 3.** Post-focal relay optical design options (unfolded versions). Arrows indicate the light path.

An alternate optical design was developed to solve these issues. The unfolded version of the alternate post-focal relay is shown in Figure 3-right. The first off-axis mirror creates a collimated beam, where the two post-focal DMs and the dichroic could be placed. The beam is then focused by a 3-mirrors assembly, including two concave mirrors and one convex mirror, which allows to control output field curvature. This design solves the issues of the phase-A baseline design. Moreover, as a by-product, the geometric distortion is even smaller: less than 0.2 milli-arcsec projected on sky over a 60 arcsec FoV, compared to 2.8 milli-arcsec of the phase-A baseline design. The main drawback of the new design is increased complexity of the mirrors aspherical figure.

## Adaptive Optics for Extremely Large Telescopes II

The folded version of the alternate post-focal relay, including DMs, dichroic and LGS refractive objective, is shown in Figure 4. The overall volume is about  $7.2 \text{ m} \times 4.3 \text{ m} \times 6.4 \text{ m}$ , considerably smaller than the phase-A baseline design volume of about  $7.4 \text{ m} \times 7.2 \text{ m} \times 8.0 \text{ m}$ .

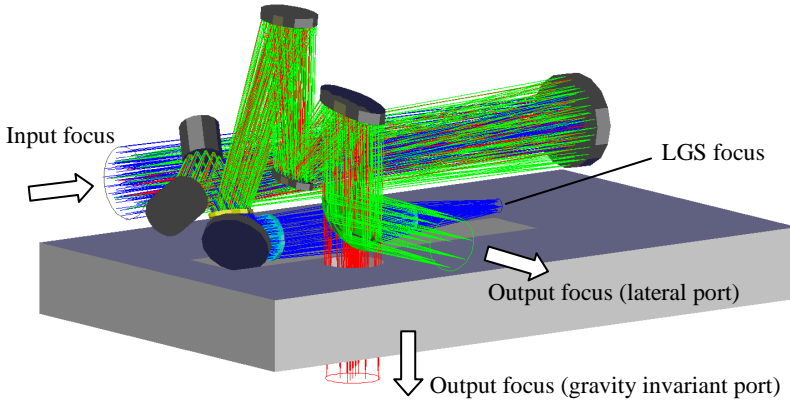


**Fig. 4.** Post focal relay alternate design layout.

MAORY implements three levels of wavefront correction: the telescope adaptive mirror M4, optically conjugated to few hundred meters above the telescope pupil and complemented by the tip-tilt mirror M5, and the two post-focal deformable mirrors, conjugated at 4 km and 12.7 km from the telescope pupil. The actuators pitch on the two post-focal DMs, projected onto the conjugate layers, is 1 m, relaxed by a factor of two with respect to the pitch of M4.

High-order wavefront sensing is performed by means of six sodium LGSs, arranged on a circle of 120 arcsec diameter. This angular separation is a good compromise between errors related to the LGS cone effect, pushing towards larger launching angles, and isoplanatic effects. The LGSs are assumed to be projected from the telescope edge: this choice translates into a slightly higher slope measurement error than central projection, due to the larger perspective spot elongation, however it allows to get rid of the so-called fratricide effect among different guide stars, related to the laser light scattering in the atmosphere. The LGS constellation is kept fixed with respect to the telescope pupil, so that it rotates with the elevation axis as seen from the Nasmyth platform. The guide stars feed six Shack-Hartmann WFS with a projected sub-aperture pitch of 0.5 m on the telescope pupil. The LGS WFS assembly has to be derotated to follow the elevation axis motion and also focused to track the sodium layer range. Each WFS probe is provided with internal focusing, to compensate the differential focus among the LGSs, and with LGS jitter compensation. The conceptual design of the LGS WFS was supported by a laboratory prototype to test critical issues related to spot elongation and sodium profile features [7, 8].

Three NGSs are used by MAORY to complement the LGS measurements [9]: as a baseline two of them are used to measure tip-tilt only, while the third, positioned on the brightest star found on the search field, is used to measure tip-tilt and focus, in order to provide a reference for the rapidly variable focus term in the LGS signals due to the sodium layer instability. The option of measuring focus by all three NGSs is also considered, as recent measurements [10]

## Adaptive Optics for Extremely Large Telescopes II

suggest that the sodium layer properties may not be the same for all LGSs. The three NGSs are searched on a wide technical FoV of 160 arcsec diameter transmitted by the post-focal relay; the three probes cannot access the central part of the field, reserved to the scientific instrument. The light beam is split in two wavelength ranges inside each NGS WFS probe: 1.5–1.8  $\mu\text{m}$  and 0.6–0.9  $\mu\text{m}$ . The infrared light (H band, 1.5–1.8  $\mu\text{m}$ ) is used for fast Tip-Tilt and Focus (TTF) measurement as previously mentioned, taking advantage of the spot shrinking ensured by the high-order correction driven by the LGS WFS, that allows the use of faint NGSs translating into high sky coverage. The NGS image shrinking also allows the windowing of the star image, providing an efficient way to reject the infrared background. The TTF NGS WFS is provided with an atmospheric dispersion compensator, as at large zenith angle the H band PSF elongation is typically 10 times larger than the E-ELT diffraction limit. The light of wavelength 0.6–0.9  $\mu\text{m}$  feeds a so-called Reference WFS, operated at temporal frequencies in the range 0.1-1 Hz and used to monitor the wavefront aberrations induced by the sodium layer features coupled with spot truncation and other effects in the LGS WFS. In normal operations the Reference WFS has a pupil sampling of approximately  $10\times 10$  subapertures. An engineering high-order wavefront sensing mode is foreseen as well.

A schematic diagram of the MCAO control system is depicted in Figure 5, showing inputs and correctors to be controlled, two inside MAORY and one integrated in the telescope (M4/M5). The baseline for the MCAO correction loop is Pseudo Open Loop Control [11], that represents a good compromise, in terms of performance and computational requirements, between an optimal approach as linear quadratic gaussian control and a plain least squares approach.

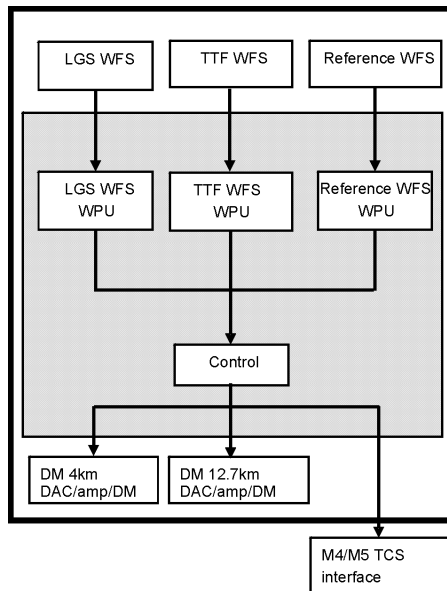


**Fig. 5.** MAORY adaptive optics system control diagram.

### 3. Adaptive optics performance

The error budget of MAORY amounts to 300 nm RMS wavefront error on average over the full 120 arcsec FoV. The error contribution allocated to the NGS WFS, accounting for measurement noise, anisoplanatism and temporal error, is 100 nm RMS corresponding to 2 milli-arcsecond angular jitter on sky.

The MCAO performance was evaluated by an analytic Fourier code [12] computing the power spectral density of the residual atmospheric turbulence phase, from which it is possible to deduce residual variance, long exposure Point Spread Function (PSF) and associated performance metrics. The Fourier code assumes implicitly infinite pupils except in the PSF calculation part, it assumes plane waves and does not incorporate LGS specific issues. These limitations were mitigated using a specific estimation of performance loss in the field induced by unseen regions associated to the combination of conic beams (spherical waves) and cylindrical beams (plane waves).

PSFs were computed using the previously mentioned tool over a grid of directions in the FoV for different wavelengths: 2.16  $\mu\text{m}$  ( $K_s$  band), 1.65  $\mu\text{m}$  (H), 1.215  $\mu\text{m}$  (J), 0.9  $\mu\text{m}$  (I). Error sources that could not be directly modelled by the Fourier code were included in the PSF calculation with an error budget approach. Figure 6 shows the Strehl Ratio (SR) as a function of the radial distance from the FoV center for “median seeing” atmospheric condition (seeing FWHM = 0.8 arcsec at 0.5  $\mu\text{m}$  wavelength and at zenith pointing,  $\tau_0 = 2.5$  ms,  $\theta_0 = 2.08$  arcsec,  $L_0 = 25$  m).

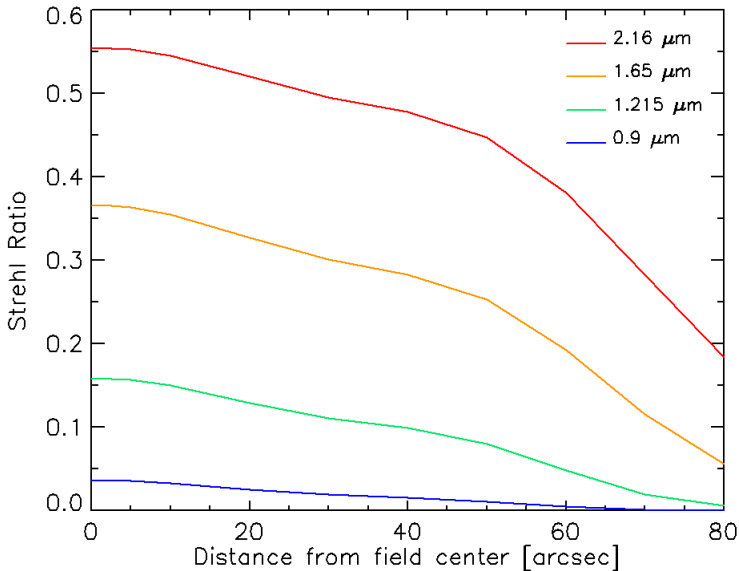


**Fig. 6.** Strehl Ratio vs. radial distance from field center.

## Adaptive Optics for Extremely Large Telescopes II

Sky coverage was estimated at the North Galactic Pole by means of Monte Carlo simulations of random asterisms with star densities derived from the TRILEGAL code [13]. Random trials were extracted, distributing the stars uniformly over the NGS search field; all the possible three star asterisms were considered, associating to each asterism a figure of merit including measurement noise, temporal error and anisoplanatic errors due to the asterism geometry and uneven brightness distribution of the NGSs. The asterism with the best figure of merit, i.e. with the lowest associated wavefront error, was chosen. The process was repeated  $\sim 1000$  times in order to have statistically significant results. Windshake, a major contributor to image jitter, was included in the calculation of the temporal error, assuming Kalman filter control.

The sky coverage of MAORY is usually expressed in terms of the fraction of sky at the North Galactic Pole where a minimum Strehl Ratio, averaged over the MICADO FoV (central  $53 \times 53$  arcsec<sup>2</sup>), can be achieved. The nominal performance shown in Figure 6 corresponds to average SR  $\sim 0.50$  at  $\lambda = 2.16 \mu\text{m}$  over the MICADO FoV. This is achieved on  $\sim 50\%$  of the sky at the North Galactic Pole. The percentage increases up to 80% if a moderate degradation of the average performance down to SR  $\sim 0.40$  at  $\lambda = 2.16 \mu\text{m}$  is accepted. These estimates are based on the assumption that all three NGS WFS measure instantaneous tip-tilt, but only one of them measures focus. As previously discussed in Section 2, all three NGS WFS may have to measure focus: sky coverage would not be significantly affected in this case.

As a concluding remark, it is interesting to notice that high sky coverage is obtained by a robust approach, where the good level of correction of the NGS images on the search field is ensured by the MCAO correction itself.

### Acknowledgement

This work was supported by the European Community (Framework Programme 6, ELT Design Study, contract No 011863; Framework Programme 7, Preparing for the Construction of the European Extremely Large Telescope, contract No INFRA-2007-2.2.1.28) and by the European Southern Observatory (Agreement No 16669/ESO/INS/07/17243/LCO).

### 4. References

1. R. Gilmozzi, J. Spyromilio, *Proceedings of the SPIE Volume 7012*, ed. L. M. Stepp, R. Gilmozzi, pp. 701219 (2008)
2. E. Diolaiti, J.-M. Conan, I. Foppiani et al., *Proceedings of the SPIE Volume 7736*, ed. B. L. Ellerbroek, M. Hart, N. Hubin, P. L. Wizinowich, pp. 77360R, (2010)
3. R. I. Davies, N. Ageorges, L. Barl et al., *Proceedings of the SPIE Volume 7735*, ed. I. S. McLean, S. K. Ramsay, H. Takami, pp. 77352A, (2010)
4. S. Ramsay, S. D'Odorico, M. Casali et al., *Proceedings of the SPIE Volume 7735*, ed. I. S. McLean, S. K. Ramsay, H. Takami, pp. 77352A, (2010)

## Adaptive Optics for Extremely Large Telescopes II

5. E. Marchetti, R. Brast, B. Delabre et al., *Proceedings of the SPIE Volume 7015*, ed. N. Hubin, C. E. Max, P. L. Wizinowich, pp. 70150F, (2008)
6. F. Rigaut et al., *This conference*, (2011)
7. M. Lombini, G. Bregoli, G. Cosentino et al., *Proceedings of the SPIE Volume 7736*, ed. B. L. Ellerbroek, M. Hart, N. Hubin, P. L. Wizinowich, pp. 77365E, (2010)
8. L. Schreiber, M. Lombini, E. Diolaiti et al., *Proceedings of the SPIE Volume 7736*, ed. B. L. Ellerbroek, M. Hart, N. Hubin, P. L. Wizinowich, pp. 77365B, (2010)
9. B. L. Ellerbroek, F. J. Rigaut, *JOSA A*, **18**, 10, pp. 2539, (2001)
10. T. Pfrommer et al., *This conference*, (2011)
11. L. Gilles, B. L. Ellerbroek, *JOSA A*, **25**, 10, pp. 2427, (2008)
12. B. Neichel, T. Fusco, J.-M. Conan, *JOSA A*, **26**, 1, pp. 219, (2008)
13. L. Girardi, M. A. T. Groenewegen, E. Hatziminaoglou, L. da Costa, *A&A*, **463**, pp. 895, (2005)